Relating the Radical Stabilization Energy and Steric Bulk of a Hydrocarbyl Group to the Strength of its Bonds with Metals and Hydrogen. A Theoretical Study

Mariusz Mitoraj,[†,‡] Hungjuan Zhu,[†] Artur Michalak,[†,‡] and Tom Ziegler*[,†]

Department of Chemistry, University of Calgary, University Drive 2500, Calgary, Alberta, Canada T2N 1N4, and Department of Theoretical Chemistry, Faculty of Chemistry, Jagiellonian University, R. Ingardena 3, 30-060 Cracow, Poland

Received January 13, 2007

We have analyzed the strength of the XR bond for a number of hydrocarbyl groups (R) attached to X = hydrogen, X = $(CNCH_3)(H)(Tp)Rh$ [Tp = H-B(pyrazolyl)$_3$], and X = $(OSi(CH_3)_3)(OSi(CH_3)_3)$-$(NH\text{-}Si(CH_3)_3)Ti$ with the help of a density functional theory (DFT) based energy decomposition scheme (EDA). The hydrocarbyl groups included had a radical sp^3 carbon with unsaturated aromatic or olefinic bonds (R^1 = Ph-CH_2, mesityl, Me-allyl, allyl) or saturated alkyl substituents (R^2 = Me, Et, Pe, i-Pr, t-Bu), a radical carbon as part of a saturated ring (R^3 = c-Pr, c-Bu, c-Pe, c-He), or a radical sp^2 carbon (R^4 = Ph, t-Bu-vinyl, Me-vinyl, vinyl). The EDA scheme was used to rationalize the relative order of the X−R^i bond energies between groups (i = 1,4), within groups (same i), and between metals X = Rh, Ti, and hydrogen (X = H). It was found that the average bond energy within each group increases as $R^4 > R^3 \sim R^2 > R^1$ for the two metals as well as H. This trend correlates with the radical stabilization energy of R^i that decreases in absolute terms as $R^4 < R^3 \sim R^1 < R^2$. This trend enables one to make rough correlations between M−C bonds and M−H links on going from one group to another. Within each of the XR^i systems where i = 1, 3, 4 there is also a correlation between the trend in the X−R^i bond energies and the R^i distortion energy. However, for the R^2 group trends in the X−R^2 bond energies are not determined by the radical stabilization but directly (X = H) or indirectly (X = Rh, Ti) by increasing steric bulk on R^2. For X = H, steric bulk directly destabilizes the H−R^2 bond by increasing the steric interaction between H and R^2 without significantly changing the H−C bond distance. For X = Rh, Ti steric bulk indirectly destabilizes the M−R^2 bond by increasing the M−C bond distance in order to relieve the steric strain. This leads to a reduction in the M−C bonding overlap and the M−C bond strength. We note finally that the Rh−R^i and Ti−R^i bonds are some 60 kcal/mol weaker than the H−R^i link. The major contributing factor here is the poorer overlap and larger energy gap between the orbitals involved in forming the M−C bond compared to the H−C link. Additional factors are larger steric interactions and the need for some distortion of the Rh and Ti fragments.

1. Introduction

The variation in the strength of C−H bonds has a profound influence on polymer chemistry, functionalization of alkanes by metalloenzymes or homogeneous catalysts, and the processing of petrochemicals. The reason(s) for the variations have been the subject of considerable controversy. This is especially the case for the series of saturated hydrocarbons H−R^2 where R^2 = Me, Et, Pr, Pe, i-Pr, and t-Bu. Experimentally, H−R^2 bond strength decreases with growing substitution on the carbon bound to hydrogen as Me > Et ∼ Pr ∼ Pe > i-Pr > t-Bu. This trend has been explained in terms of increasing stabilization of the R^2 radical with growing substitution on the radical carbon. However recently Gronert[1] has provided evidence for an explanation of the trend in terms of growing 1,3 geminal repulsion between hydrogen and the substituents on the carbon bound to hydrogen. This notion has been supported by a study due to Mitoraj et al.[2] in which use was made of a density functional theory (DFT) based energy decomposition scheme.[3]

The determination[4] of M−H and M−C bond energies is as essential to organometallic chemistry[5−11] as the measurement of C−H and C−C bond enthalpies[12] has been to organic chemistry. However, the experimental challenges have been considerable, and it is only slowly over the past 20 years that an accurate database[4,13−15] for M−H and M−C bond energies

* Corresponding author. E-mail: ziegler@ucalgary.ca.
† University of Calgary.
‡ Jagiellonian University.

(1) Gronert, S. *J. Org. Chem.* **2006**, *71*, 1209−1219.
(2) Mitoraj, M.; Zhu, H.; Michalak, A.; Ziegler, T. *J. Org. Chem.* **2006**, *71*, 9208−9211.
(3) Ziegler, T.; Rauk, A. *Inorg. Chem.* **1979**, *18*, 1755−1759.
(4) Martinho-Simoes, J. A.; Beauchamp, J. L. *Chem. Rev.* **1990**, *90*, 629−688.
(5) Crabtree, R. H. *Chem. Rev.* **1985**, *85*, 245−269.
(6) Graham, W. A. G. *J. Organomet. Chem.* **1986**, *300*, 81−89.
(7) Arndsten, A. B.; Bergman, R. G.; Mobley, T. A.; Peterson, H. T. *Acc. Chem. Res.* **1995**, *28*, 154−162.
(8) Shilov, A. E.; Shul'pin, G. B. *Chem. Rev.* **1997**, *97*, 2879−2932.
(9) Labinger, J. A.; Bercaw, J. E. *Nature* **2002**, *417*, 507−514.
(10) Jones, W. D. *Acc. Chem. Res.* **2003**, *36*, 140−146.
(11) Hoff, C. D. *Prog. Inorg. Chem.* **1992**, *40*, 503−61.
(12) *Handbook of Chemistry and Physics*, 84th ed.; Lide, D. R., Ed.; CRC Press: Boca Raton, FL, 2004.
(13) Lersch, M.; Tilset, M. *Chem. Rev.* **2005**, *105*, 2471−2526.

10.1021/om0700361 CCC: $37.00
Publication on Web 02/23/2007

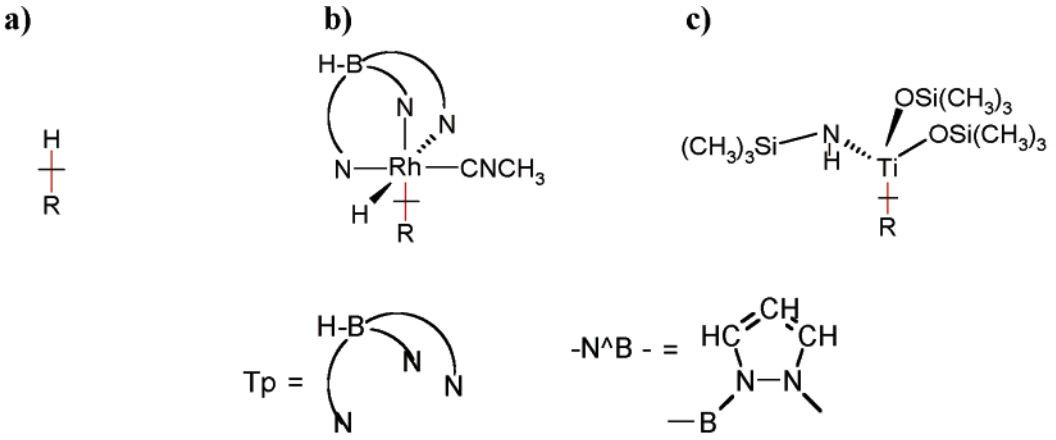

Figure 1. Schematic representation of the systems studied in the present work: the hydrocarbons (a), the rhodium (b), and the titanium complexes (c).

of coordinatively saturated organometallics has emerged. Unfortunately, the database is not yet large enough to estimate routinely the heat of reaction for the addition of a C−C or C−H bond to any metal center M with sufficient accuracy. This is perhaps not surprising given the large number of possible combinations. Nevertheless, a certain pattern of systematics seems to be emerging[16−23] that might help in making useful interpolations. Theoretical methods based on DFT[24,25] as well as high-level *ab initio* methods[24−27] have also been used to investigate M−C and M−H bond strengths. Experience has shown that only high-level *ab initio* methods[24,25] in conjunction with extensive basis sets can afford M−H and M−C bond energies with an accuracy of 1−2 kcal/mol. Nevertheless useful thermodynamic and kinetic studies can be carried out by DFT-based methods.[28−30]

Among the interesting patterns in M−C bond energies is the correlation between C−H and M−C bonds strength. This correlation was first explored by Bryndza[16] and later taken up in extensive investigations by Jones[20,21] for Rh−C bonds and Wolczanski[22,23] for Ti−C links. Most recently Clot et al.[31] extended the correlation between C−H and Rh−C/Ti−C bonds in a computational investigational that prompted our study.

We shall here in the first place make use of our DFT-based bond energy decomposition scheme[3,29] to extend the recent investigation[2] of C−H bonds in saturated hydrocarbons involving H−R^2 where R^2 = Me, Et, Pe, i-Pr, and t-Bu to other types of H−R links. The extension will be to cases where hydrogen is bound to an sp^3 carbon with substituents containing unsaturated aromatic or olefinic bonds (R^1 = Ph-CH_2, mesityl, Me-allyl, allyl), a carbon as part of a saturated ring (R^3 = c-Pr, c-Bu, c-Pe, c-He), or an sp^2 carbon (R^4 = Ph, t-Bu-vinyl, Me-vinyl, vinyl). The objective here is to explore how steric and electronic factors determine the order in the H−C bond strength through the H−R^i series (i = 1,4). The second objective will be to extend the bond decomposition study to the corresponding M−R^i series (i = 1,4) with M = Rh, Ti by making use of the same simplified models of metal complexes as explored computationally by Clot et al.[31] (Rh, Ti), which were based on the systems studied experimentally by Jones et al.[20,21] (Rh) as well as Wolczanski et al.[22,23] (Ti). We hope here to explore factors of importance for M−C bond strength and the way these factors influence the possible correlation[20,22,31] between M−C/H−C bond enthalpies.

2. Computational Details and Models

A schematic representation of the systems studied in the present work is given in Figure 1. All the calculations were performed with the Amsterdam Density Functional (ADF) package, version 2005.04.[32,33] The bonding interactions between the radical fragments H and R in Figure 1a, $(CNCH_3)(H)(Tp)$-Rh [Tp = H−B(pyrazolyl)$_3$] and R in Figure 1b, and $(OSi(CH_3)_3)(OSi(CH_3)_3)(NH-Si(CH_3)_3)$-Ti and R in Figure 1c were analyzed with the energy decomposition method (EDA) developed by Ziegler and Rauk.[3,29]

(14) Armentrout, P. B. *Organometallic Bonding and Reactivity*; Brown, J. M., Hofmann, P., Eds.; *Topics in Organometallic Chemistry*, Vol. 4; Springer-Verlag: Berlin, 1999; pp 1−45.
(15) Hall, C.; Perutz, R. N. *Chem. Rev.* **1996**, *96*, 3125−3146.
(16) Bryndza, H. E.; Fong, L. K.; Paciello, R. A.; Tam, W.; Bercaw, J. E. *J. Am. Chem. Soc.* **1987**, *109*, 1444−1456.
(17) Holland, P. L.; Andersen, R. A.; Bergman, R. G.; Huang, J. K.; Nolan, S. P. *J. Am. Chem. Soc.* **1997**, *119*, 12800−12814.
(18) Holland, P. L.; Andersen, R. A.; Bergman, R. G. *Comments Inorg. Chem.* **1999**, *21*, 115.
(19) Schultz, A. J.; Williams, J. M.; Schrock, R. R.; Rupprecht, G. A.; Fellmann, J. D. *J. Am. Chem. Soc.* **1979**, *101*, 1593−1595.
(20) Jones, W. D.; Hessel, E. T. *J. Am. Chem. Soc.* **1993**, *115*, 554−562.
(21) Wick, D. D.; Jones, W. D. *Organometallics* **1999**, *18*, 495−505.
(22) Bennett, J. L.; Wolczanski, P. T. *J. Am. Chem. Soc.* **1994**, *116*, 2179−2180.
(23) Bennett, J. L.; Wolczanski, P. T. *J. Am. Chem. Soc.* **1997**, *119*, 10696−10719.
(24) Siegbahn, P. E. M. *J. Phys. Chem.* **1995**, *99*, 12723−12729.
(25) Zhao, Y.; Lynch, B. J.; Truhlar, D. G. *J. Phys. Chem. A* **2005**, *108*, 4786−4791.
(26) Henry, D. J.; Parkinson, C. J.; Mayer, P. M.; Radom, L. *J. Phys. Chem. A* **2001**, *105*, 6750−6756.
(27) Izgorodina, E. I.; Coote, M. L.; Radom, L. *J. Phys. Chem. A* **2005**, *109*, 7558−7566.
(28) Ziegler, T. *Chem. Rev.* **1991**, *91*, 651−667.
(29) Ziegler, T.; Autschbach J. *J. Chem. Rev.* **2005**, *105*, 2695−2722.
(30) Niu, S. Q.; Hall, M. B. *Chem. Rev.* **2000**, *100*, 353−406.
(31) Clot, E.; Megret, C.; Eisenstein, O.; Perutz, R. N. *J. Am. Chem. Soc.* **2006**, *128*, 8350−8357.
(32) Guerra, F.; Visser, O.; Snijders, J. G.; te Velde, G. Baerends, E. J. In *Methods and Techniques in Computational Chemistry*; Clementi, E., Corongiu, G., Eds.; METACC-9, STEF: Cagliari, 1995; pp 303−395.
(33) TeVelde, G.; Bickelhaupt, F. M.; Baerends, E. J.; Fonseca Guerra, C.; van Giesbergen, S. J.; Snijders, J. G.; Ziegler, T. *J. Comput. Chem.* **2001**, *22*, 931−967.

Table 1. Total Calculated H−C, Rh−C,[d] and Ti−C[d] Bond Energies,[b,c] ΔE_{bond}^{tot}

ligand[a]	H−C	Rh−C	Ti−C
R^1			
Ph-CH_2	−94.12	−42.87	−46.75
mesityl	−93.94	−42.18	
Me-allyl	−92.86	−41.32	−43.74
allyl	−91.36	−40.72	
R^2			
Me	−110.52	−54.81	−56.94
Pr	−106.51	−55.49	−52.67
Et	−106.67	−51.80	−52.16
Pe	−106.40	−51.70	
i-Pr	−103.15	−46.76	−48.42
t-Bu	−100.32	−41.33	−45.29
R^3			
c-Pr	−112.39	−59.44	−62.44
c-Bu	−104.06	−51.25	−50.87
c-Pe	−100.30	−45.86	−46.57
c-He	−103.03	−47.42	−48.63
R^4			
Ph	−115.97	−68.25	−64.91
Me-vinyl	−116.42	−66.28	
vinyl	−115.13	−66.95	−64.55
t-Bu-vinyl	−114.67	−64.75	

[a] For definition of ligands see text. [b] For a definition of ΔE_{bond}^{tot} see eq 1. [c] Energies in kcal/mol. [d] For definition of Rh and Ti complexes see Figure 1.

Use was made of a nonlocal exchange−correlation functional (BP86) due to Becke[34] and Perdew.[35] A double-ζ quality basis of Slater-type atomic orbitals (STO) with one set of polarization functions was employed for H, C, N, O, B, and Si atoms, and a triple-ζ basis was used for the Rh and Ti atoms. The 1s electrons of the atoms C, N, O, and B as well as the 1s-4p shells of Rh, the 1s-3p levels of Ti, and the 1s-2p electrons of Si were treated as frozen core. All the presented energies include first-order scalar relativistic corrections.[33] Finally, a bond order analysis was performed based on the Nalewajski−Mrozek methodology.[36] The geometries of all the species discussed here were taken from Clot et al.[31] in order to have a direct correspondence with the results of ref 31, obtained with different computational details. Such geometries do not correspond to the minima on the BP86 potential energy surface. Therefore, to test the errors introduced by the nonoptimized geometries, we have performed the geometry optimization for the six examples of complexes. All the bond energy differences are below 1 kcal/mol. Therefore, the lack of geometry optimization in our calculations does not change the major conclusions drawn in this paper. The bond energies presented in Table 1 are electronic enthalpies only since our interest is in an analysis of this component through the EDA scheme.[3,29] The total bond energy should in addition contain a zero-point energy correction as well as finite temperature terms that primarily take into account that a M−C or H−C stretching frequency is lost on X−C bond fission. These corrections amount to 4−6 kcal/mol for H−C bonds and 1−3 kcal/mol for M−C bonds. Clot et al.[31] have shown that electronic enthalpies based on the BP86 functional used here in conjunction with the corrections mentioned above afford total bond enthalpies in good agreement with experiment.

3. Results and Discussion

Let us first present the basic concepts of the EDA (energy decomposition method).[3,29] In this scheme, the total bonding energy between the interacting fragments (ΔE_{bond}^{tot}) is divided into four components (eq 1):

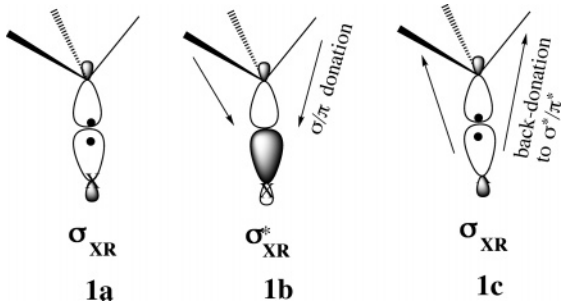

$$\Delta E_{bond}^{tot} = \Delta E_{dist} + [\Delta E_{elstat} + \Delta E_{Pauli}] + \Delta E_{orbital} = \Delta E_{dist} + \Delta E_{steric} + \Delta E_{orbital} \quad (1)$$

The first component, referred to as the total distortion term, ΔE_{dist}, represents the amount of energy required to promote the separated fragments from their equilibrium geometry to the structures they will take up in the combined molecule. The distortion energy term can be further divided into two components for the rhodium and titanium systems. The first one gives the hydrocarbyl (R) distortion energy contribution, $\Delta E_{dist}^{R(X)}$, and the second one, $\Delta E_{dist}^{Rh-frag}$ or $\Delta E_{dist}^{Ti-frag}$, describes the metal-fragment distortion energy. Their sum ($\Delta E_{dist}^{R(X)} + \Delta E_{dist}^{Rh-frag}$ or $\Delta E_{dist}^{R} + \Delta E_{dist}^{Ti-frag}$) gives the total distortion term, ΔE_{dist} or ΔE_{dist}^{RX}. The second term, ΔE_{elstat}, in eq 1 corresponds to the classical electrostatic interaction between the promoted fragments. The third term, ΔE_{Pauli}, accounts for the repulsive Pauli interaction between occupied orbitals on the two fragments. The sum $\Delta E_{elstat} + \Delta E_{Pauli}$ is referred to as the steric repulsion term, ΔE_{steric}, between the two fragments.

Finally, the last term, $\Delta E_{\text{orbital}}$, represents the interactions between the occupied molecular orbitals on one fragment with the unoccupied molecular orbitals of the other fragment as well as mixing of occupied and virtual orbitals within the same fragment (inner-fragment polarization). The term $\Delta E_{orbital}$ is, for the sake of interpretation, calculated in two steps. In the first step we evaluate $\Delta E_{radical}^{orb}$ as $\Delta E_{orbital}$ from a calculation of XR where we have deleted all virtual orbitals on X and R except the X- and R-SUMOs. The first terms ($\Delta E_{radical}^{orb}$) represents primarily the formation of the σ_{XR} bonding orbital from the radical interaction between the singly occupied carbon-based orbital on R (R-SOMO) and the singly unoccupied orbital (X-SUMO) on H, Rh, or Ti, **1a** , as well as the interaction between the singly unoccupied orbital on carbon (R-SUMO) and the singly unoccupied orbital on H, Rh, or Ti, **1a**. However, it contains also donation of charge from the occupied orbitals (σ or π) on R to the antibonding σ^*_{XR} orbital, **1b**. The second contribution ($\Delta E_{virtual}^{orb}$) to $\Delta E_{orbital}$ is the further stabilization we gain by including all additional virtual orbitals on R and X in the calculations. An analysis reveals that $\Delta E_{virtual}^{orb}$ primarily comes from (back-) donation of charge from σ_{XR} to empty (σ^* or π^*) orbitals on R, **1c**. The RH hydrocarbons as well as the rhodium[20,21] and titanium[22,23] alkyl complexes shown in Figure 1 have been the subject of both experimental and theoretical studies. Of special interest has been the correlation established by both theory[31] and experiment[16,20,23] between H−R bond energies on one hand and Rh−R or Ti−R bond strengths on the other. We shall in the current study make use of DFT and eq 1 in order to understand what factors (steric or electronic) might be responsible for such a correlation. The theoretical work

(34) Becke, A. *Phys. Rev. B* **1988**, *38*, 3098−3100.
(35) Perdew, J. P. *Phys. Rev. B* **1986**, *33*, 8822−8824.
(36) Nalewajski, R. F.; Mrozek, J.; Michalak, A. *Int. J. Quantum Chem.* **1997**, *61*, 589−601.

Table 2. Contribution from Orbital Interaction Terms[a,b] $\Delta E_{orbital}$, $\Delta E^{orb}_{radical}$, and $\Delta E^{orb}_{virtual}$ to the C−H, Rh−C, and the Ti−C Bond Energies

	C−H			Rh−C			Ti−C		
ligand[c]	$\Delta E^{orb}_{radical}$	$\Delta E^{orb}_{virtual}$	$\Delta E_{orbital}$	$\Delta E^{orb}_{radical}$	$\Delta E^{orb}_{virtual}$	$\Delta E_{orbital}$	$\Delta E^{orb}_{radical}$	$\Delta E^{orb}_{virtual}$	$\Delta E_{orbital}$
R^1									
Ph-CH_2	−129.32	−34.73	−164.05	−85.58	−20.84	−106.42	−84.58	−28.44	−113.02
mesityl	−129.40	−32.74	−162.14	−85.06	−21.04	−106.10			
Me-allyl	−125.60	−30.95	−156.55	−83.63	−20.29	−103.92	−81.81	−29.39	−111.20
allyl	−126.43	−32.45	−158.88	−85.18	−20.14	−105.32			
R^2									
Me	−117.54	−20.60	−138.14	−89.10	−13.66	−102.76	−84.40	−20.82	−105.22
Pr	−119.61	−20.85	−140.46	−87.57	−17.78	−105.35	−83.95	−22.60	−106.55
Et	−120.49	−21.29	−141.78	−86.81	−15.09	−101.90	−83.18	−22.44	−105.62
Pe	−121.12	−21.59	−142.71	−87.14	−15.47	−102.61			
i-Pr	−121.81	−22.35	−144.16	−79.52	−19.32	−98.84	−80.54	−22.99	−103.53
t-Bu	−122.35	−23.99	−146.34	−76.90	−18.43	−95.34	−77.93	−23.35	−101.28
R^3									
c-Pr	−126.39	−22.04	−148.43	−91.80	−17.92	−109.72	−89.61	−25.24	−114.86
c-Bu	−123.33	−22.30	−145.63	−85.57	−18.29	−103.86	−82.38	−24.94	−107.31
c-Pe	−122.81	−22.09	−144.90	−85.09	−18.07	−103.16	−82.67	−24.51	−107.18
c-He	−120.00	−21.63	−141.63	−82.86	−17.81	−100.67	−81.67	−24.10	−105.66
R^4									
Ph	−128.51	−19.84	−148.35	−94.59	−22.93	−117.52	−90.43	−23.59	−114.02
Me-vinyl	−125.60	−20.89	−146.49	−97.27	−20.30	−117.57			
vinyl	−126.23	−21.28	−147.51	−97.80	−20.87	−118.67	−91.14	−23.95	−115.09
t-Bu-vinyl	−126.64	−21.76	−148.40	−96.86	−20.52	−117.38			

[a] Energies in kcal/mol [b] $\Delta E_{orbital}$, $\Delta E^{orb}_{radical}$, $\Delta E^{orb}_{virtual}$ are defined in the text near eq 1. [c] For definition of ligands see text. [d] For definition of Rh and Ti complexes see Figure 1. [e] $\Delta E_{orbital} = \Delta E^{orb}_{radical} + \Delta E^{orb}_{virtual}$.

by Clot et al.[31] as well as the experimental studies by Jones,[20,21] Bennett,[22,23] and Bryndza[16] involves a large number of R groups. We shall start with those R groups that are bound to X through an sp^3 carbon with unsaturated substituents (R^1 = Ph-CH_2, mesityl, Me-allyl, allyl).

The R^1 Series (R^1 = Ph-CH_2, mesityl, Me-allyl, allyl). The R^1 series **2** forms X−R^1 bonds (X = H, Rh, Ti) that are weaker than the corresponding X−R^i links involving i = 2, 4 (Table 1) because more energy is required to distort a radical in R^1 from its ground state state to the geometry it has in XR^1 than for radicals in any other group. The larger distortion energies calculated for R^1 compared to R^i (i = 2, 4) reflect the fact that the R^1 radicals **2** all are planar with substantial delocalization (hyperconjugation) of the unpaired electron into the π^* aryl or olefin orbitals. Much of this stabilization is lost when R^1 is pyramidalized in the X−R^1 complex.

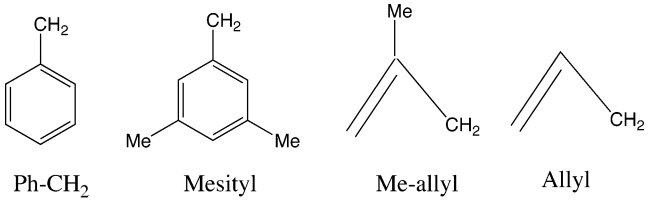

2

In Figure 2 are correlated the distortion energy for R^i in XR^i ($\Delta E^{R(X)}_{dist}$) against the total X−R^i bond energy (ΔE^{tot}_{bond}) for i = 1, 4 with X = H (Figure 2a), X = Rh (Figure 2b), and X = Ti (Figure 2c). We find for X = H, Rh, and Ti that the XR^1 systems in Figures 2a−c at the top right position are among the complexes with the weakest X−C bond and the largest distortion energy, $\Delta E^{R(X)}_{dist}$. The R^1 series also experience the largest steric destabilization among the four groups for X = H. However this is compensated for by a corresponding larger stabilization from $\Delta E_{orbital}$. The reason for this is that the π orbitals in R^1 are especially effective in donating density to σ^*_{XR}, **1b**, ($\Delta E^{orb}_{radical}$). At the same time π^* orbitals on R^1 are efficient at accepting density from σ_{XR} ($\Delta E^{orb}_{virtual}$), **1c**; see Table 2.

The trend in the X−R^1 bond strengths is Ph-CH_2 > mesityl > Me-allyl > allyl, Table 1. This is the opposite of what we find (and would expect) on steric grounds, Table 4. The highest values of total Pauli repulsion terms are observed for the R^1 group, which results in the highest positive values of the steric repulsion terms ΔE_{steric}. The trend is, however, in line with $-\Delta E_{orbital}$, where we find Ph-CH_2 ∼ mesitylene > Me-allyl ∼ allyl, Table 2. Apparently, the larger number of π and π^* orbitals on Ph-CH_2 and mesitylene compared to Me-allyl and allyl renders $\Delta E_{orbital}$ more stabilizing for the first group in R^1 through the donation, **1b**, and back-donation, **1c**, processes. Finally, within the XR^1 series there is a reasonable correlation between the X−R^1 bond energy and $\Delta E^{R(X)}_{dist}$ such that ΔE^{tot}_{bond} decreases

Table 3. H−X Distances R(H−X)[a] and Bond Orders BO(H−X)[b].

	H−C		Rh−C		Ti−C	
ligand	R(H−C)	B(H−C)	R(Rh−C)	B(Rh−C)	R(Ti−C)	B(Ti−C)
R^1						
Ph-CH2	1.097	1.032	2.095	0.927	2.113	0.829
mesityl	1.096	1.034	2.095	0.928		
Me-allyl	1.097	1.030	2.096	0.923	2.107	0.841
allyl	1.097	1.032	2.091	0.921		
R^2						
Me	1.092	1.081	2.065	1.076	2.084	0.979
Pr	1.096	1.036	2.074	0.969	2.089	0.942
Et	1.095	1.039	2.074	0.961	2.088	0.945
Pe	1.095	1.042	2.074	0.969		
i-Pr	1.098	0.993	2.104	0.844	2.096	0.908
t-Bu	1.100	0.942	2.141	0.725	2.107	0.860
R^3						
c-Pr	1.086	0.993	2.047	0.958	2.061	0.922
c-Bu	1.094	0.985	2.067	0.759	2.080	0.917
c-Pe	1.095	0.981	2.081	0.747	2.082	0.918
c-He	1.100	0.966	2.100	0.743	2.093	0.913
R^4						
Ph	1.086	0.988	2.032	0.817	2.090	0.870
Me-vinyl	1.086	1.027	2.010	0.926		
vinyl	1.087	1.020	2.007	0.918	2.074	0.912
t-Bu-vinyl	1.086	1.026	2.014	0.921		

[a] Ref 31. [b] Ref 36. [c] For definition of ligands see text. [d] For definition of Rh and Ti complexes see Figure 1.

Table 4. Contribution from Steric Repulsion,[a,b] ΔE_{steric}, to the H−X, Rh−C,[d] and Ti−C Bond Energies

ligand[c]	C−H	Rh-C	Ti−C
R^1			
Ph-CH2	54.95	43.53	46.72
mesityl	51.79	43.81	
Me-allyl	45.72	42.14	47.40
allyl	48.56	43.40	
R^2			
Me	18.35	35.69	32.55
Pr	24.92	36.65	38.38
Et	26.12	37.40	38.31
Pe	26.98	37.68	
i-Pr	32.15	37.27	39.98
t-Bu	37.32	36.70	40.39
R^3			
c-Pr	30.21	39.76	38.31
c-Bu	32.26	38.09	40.22
c-Pe	31.62	37.54	40.62
c-He	29.63	38.62	41.17
R^4			
Ph	27.94	38.97	34.55
Me-vinyl	25.24	41.36	
vinyl	26.98	42.12	36.22
t-Bu-vinyl	27.85	42.41	

[a] Energies in kcal/mol. [b] ΔE_{steric} is defined in the text near eq 1. [c] For definition of ligands see text. [d] For definition of Rh and Ti complexes see Figure 1.

with $\Delta E_{dist}^{R(X)}$, Table 5 and Figure 2. Here the loss in delocalization energy for the unpaired electron on pyramidalization of R^2 is larger for the allyl systems than the benzyl group.

The R^3 Series (R^3 = c-Pr, c-Bu, c-Pe, c-He). In the XR^3 series to be discussed next, X is bound to a carbon atom that is part of a more or less strained alkyl ring (R^3 = c-Pr, c-Bu, c-Pe, c-He), **3**.

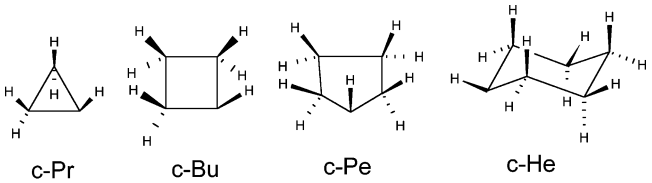

3

The formal hybridization in the carbon σ-orbital participating in σ_{XR} goes gradually from sp^2 for R^3 = c-Pr to sp^3 for R^3 = c-He, as the ring strain is reduced. In terms of X−R bond energies, this group fills the gap between the R^1 and R^4 series. Thus c-Pr, which has the lowest value for $\Delta E_{dist}^{R(X)}$ and an sp^2 hybridization around the radical carbon, has a strong X−C bond similar to those in the XR^4 series with pure sp^2 hybridization. On the other hand R^3 = c-Pe with an sp^3 hybridization and the highest distortion energy has a weak X−C bond close to those in the XR^1 series, Figure 2.

Within the XR^3 series one trend setting factor for the $X-R^3$ bond energies is $-\Delta E_{radical}^{orb}$. It is seen to decrease from R^3 = c-Pr to R^3 = c-He as the hybridization of the carbon lobe in σ_{XR} changes from sp^2 to sp^3. The change in hybridization reduces the bonding overlap in σ_{XR}. Associated with the decrease in bond strength is a lengthening of the $X-R^3$ bond distance for X = H and especially X = Ti, Rh, Table 3. It follows further from Figure 2 and Table 5 that within the XR^3 series there is a reasonable correlation between $\Delta E_{dist}^{R(X)}$ and ΔE_{bond}^{tot}, as in the case of the XR^1 group.

The calculated $X-R^3$ bond energies in three- to six-membered rings (c-Pr, c-Bu, c-Pe, c-He) are close to experimental data, within the experimental error bars.[22] From our calculations we find the C−H bond energies for c-Pe to be 2.7 kcal/mol greater than the C−H bond energy for c-He. In agreement with our findings, a recent G3 calculation[37] also finds c-Pe to form a weaker C−H bond than c-He by 3.2 kcal/mol. The reason for the low theoretical estimate of the C−H bond strength in the case of c-Pe is the fact that we calculate $\Delta E_{dist}^{R(X)}$ to be 4 kcal/mol higher for c-Pe than for either c-He or c-Bu.

For $X-R^3$ with X = Ti, Rh we find again that $\Delta E_{dist}^{R(X)}$ is higher (4−5 kcal/mol) for c-Pe than for either c-He or c-Bu. The high value for $\Delta E_{dist}^{R(X)}$ in the case of c-Pe reflects a substantial rearrangement in the c-Pe fragment as it goes from the radical state to the X(c-Pe) compound. This results in the weaker Rh−C and Ti−C bonds for the c-Pe substituent.

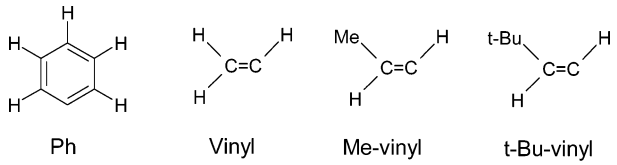

4

The R^4 Series (R^4= Ph, Me-vinyl, vinyl, t-Bu-vinyl). The next series is R^4 = Ph, Me-vinyl, vinyl, and t-Bu-vinyl, where the radical carbon is sp^2 hybridized. It follows from Table 1 that $X-R^4$ bonds are stronger than their $X-R^i$ counterparts (i = 1, 3). Of importance here is the modest contributions from $\Delta E_{dist}^{R(X)}$ for X = H, Rh, and Ti and from ΔE_{steric} for X = H. Thus not much rearrangement is required of the R^4 radical to form an $X-R^4$ bond, and the steric bulk of R^4 is restricted to one plane. It follows from Figure 2 that the XR^4 systems are positioned at the left bottom corner among the systems with the strongest X−C bond energies and the lowest values for $\Delta E_{dist}^{R(X)}$.

The R^2 Series (R^2= Me, Et, Pr, Pe, i-Pr, and t-Bu). The last group to be discussed is the sp^3 series R^2. Where R^1 had unsaturated aryl or olefin bonds, R^2 has saturated alkyl groups (or hydrogen atoms) as substituents. In terms of C−X bond strengths the XR^2 series forms stronger C−X links than XR^1. One important contributing factor to this is $\Delta E_{dist}^{R(X)}$, which (on average) is larger for R^1 than for R^2, Table 5. We can understand this by noting that the loss of hyperconjugation on pyramidalization in R^2 involves the less effective donation into σ^* alkyl orbitals rather than delocalization into π^* as in R^1. The position of the average $X-R^2$ bond energy in Figure 2 correlates well with the average $\Delta E_{dist}^{R(X)}$ value for XR^2 donation. However, it is evident from Figure 2 and Tables 1 and 5 that the trend within the XR^2 group is not primarily determined by $\Delta E_{dist}^{R(X)}$.

It follows from Table 1 that the calculated $H-R^2$, $Ti-R^2$, and $Rh-R^2$ bond energies in absolute terms decrease through the series R^2 = Me, Pr, Et, Pe, i-Pr, t-Bu. This trend is in agreement with experiment[12] and previous calculations[1,2,31] on the HR^2 systems. We should point out that the results obtained by Clot et al.[31] are in slightly better agreement with experimental data,[12] due to the methodology differences (basis sets, XC functionals). For $Ti-R^2$ and $Rh-R^2$ our calculations agree as far as the trends are concerned with previous theoretical studies[31] and somewhat more limited experimental data.[20,22] The only exception is the Rh−Pr bond, which we find to be slightly more stable than the Rh−Me link. We note for X = H that $\Delta E_{radical}^{orb}$ becomes more stabilizing through the series R^2 as the number

(37) Bach, R. D.; Dmitrenko, O. *J. Am. Chem. Soc.* **2004**, *126*, 4444−4452.

Table 5. Total Distortion Energy,[a] ΔE_{dist}, Together with the Contributions $\Delta E_{dist}^{R(X)}$, $\Delta E_{dist}^{Rh-frag}$, and $\Delta E_{dist}^{Ti-fragment}$

	H−C	Rh−C			Ti−C		
ligand	$\Delta E_{dist}^{R(H)\,b,i}$	$\Delta E_{dist}^{R(Rh)\,c}$	$\Delta E_{dist}^{Rh-frag\,d}$	$\Delta E_{dist}^{RhR\,e}$	$\Delta E_{dist}^{R(Ti)\,f}$	$\Delta E_{dist}^{Ti-frag\,g}$	$\Delta E_{dist}^{TiR\,h}$
R^1							
Ph−CH_2	12.18	14.73	3.31	18.04	10.59	7.46	18.05
mesityl	13.65	14.90	3.27	18.17			
Me-allyl	15.28	15.40	3.29	18.69	11.27	7.43	18.70
allyl	16.28	16.21	3.23	19.44			
R^2							
Me	7.32	8.51	3.00	11.51	8.16	7.24	15.40
Pr	6.80	8.51	2.90	11.41	7.46	6.52	13.98
Et	6.78	8.44	2.83	11.27	7.39	6.47	13.86
Pe	7.04	8.63	2.93	11.56			
i-Pr	6.55	9.59	3.22	12.81	7.25	6.12	13.37
t-Bu	6.27	11.10	3.87	14.97	7.32	6.12	13.44
R^3							
c-Pr	3.39	5.17	3.14	8.31	5.21	6.97	12.18
c-Bu	6.90	9.04	2.94	11.98	7.90	6.53	14.43
c-Pe	10.57	14.18	2.94	17.12	11.32	6.55	17.87
c-He	6.61	8.79	3.07	11.86	7.38	6.36	13.74
R^4							
Ph	1.78	3.87	3.40	7.27	3.65	8.20	11.85
Me-vinyl	2.91	4.70	3.05	7.75			
vinyl	2.82	4.55	3.04	7.59	5.00	7.51	12.51
t-Bu-vinyl	3.20	4.91	3.10	8.01			

[a] Energies in kcal/mol. [b] $\Delta E_{dist}^{R(H)}$: distortion energy of R fragment in HR. [c] $\Delta E_{dist}^{R(Rh)}$: distortion energy of R fragment in RhR. [d] $\Delta E_{dist}^{Rh-frag}$: distortion energy of Rh fragment in RhR. [e] $\Delta E_{dist}^{RhR} = \Delta E_{dist}^{R(Rh)} + \Delta E_{dist}^{Rh-frag}$: total distortion energy in RhR. [f] $\Delta E_{dist}^{R(Rh)}$: distortion energy of R fragment in TiR. [g] $\Delta E_{dist}^{Ti-frag}$: distortion energy of Ti fragment in TiR. [h] $\Delta E_{dist}^{TiR} = \Delta E_{dist}^{R(Ti)} + \Delta E_{dist}^{Ti-frag}$: total distortion energy in TiR. [i] $\Delta E_{dist}^{HR} = \Delta E_{dist}^{R(H)}$: total distortion energy in HR.

of occupied σ orbitals increases that can donate density into the σ^*_{XR}, **1b**. At the same time the number of σ orbitals on R^2 increases that can receive density from σ_{XR}, **1c**, resulting in further stabilization through the series H−R^2 from $\Delta E_{virtual}^{orb}$. All together $\Delta E_{orbital}$ is seen to stabilize the H−R^1 bond from Me to t-Bu. The orbital interaction energies $\Delta E_{orbital}$ decomposed into $\Delta E_{radical}^{orb}$ and $\Delta E_{virtual}^{orb}$ are shown in Table 2.

Table 4 displays the steric interaction energy, ΔE_{steric}. For H−R^2 the repulsive interaction between H and R^2 increases with steric bulk on R^2. In fact ΔE_{steric} becomes the trend setting term for the H−R^2 bond energies, as already suggested by Gronert[1] and demonstrated by us[2] in a previous theoretical study. We note that the H−C bond distance in H−R^2 is nearly the same from Me (1.092 Å) to t-Bu (1.100 Å), Table 3. Thus, in H−R^2 the increasing steric interaction is not relived by increasing the H−C bond distance. The trends in the H−R^2 bond energies have often been explained in terms of the relaxation energy gained by R^2 after it has dissociated from H. We present in Table 5 the energy $\Delta E_{dist}^{R(H)}$ required to distort R^2 from its ground state to the geometry it has in HR^2. From this distortion energy we can obtain the radical relaxation energy as $-\Delta E_{dist}^{R(H)}$. It is clear from Table 5 that the radical relaxation energy hardly changes from Et to t-Bu. It can thus not be responsible for the trend in the H−R^2 bond energy.[3,37]

We shall now turn to X = Rh, Ti. Here the potential for increasing steric interaction between X = Rh, Ti, and R^2 gives rise to an elongation of the X−R^2 bond (Table 3) with the result that the overlaps in σ_{XR} between the X-SOMO and the R^2-SUMO as well as the X-SUMO and the R^2-SOMO, **1a**, are reduced. As a result, $\Delta E_{radical}^{orb}$ and $\Delta E_{orbital}$ are seen to decrease in absolute terms from Me to t-Bu, Table 2. The relief in steric strain through an increase in the Ti−R^2 and Rh−R^2 distances results in a situation where ΔE_{steric} hardly changes through the series Et to t-Bu. Thus, the steric interaction does not directly set the trend for the bond energies in the Ti−R^2 and Rh−R^2 systems. This trend is instead set by $\Delta E_{radical}^{orb}$. However $\Delta E_{radical}^{orb}$ is indirectly influenced by the increasing steric bulk from Me to t-Bu as discussed previously.

We note finally that the Rh−R^2 and Ti−R^2 bonds are some 60 kcal/mol weaker than the H−R^1 link. There are three factors contributing to this difference, namely, $\Delta E_{orbital}$ (~56%), ΔE_{steric} (~28%), and $\Delta E_{dist}^{Rh-frag}$ or $\Delta E_{dist}^{Ti-frag}$ (~16%). The difference between the Rh−R^2 and Ti−R^2 bond energies is, on the other hand, marginal. The more modest stabilization in $\Delta E_{orbital}$ for X = Ti, Rh compared to X = H stems from the fact that the orbitals involved in the formation of σ_{XR} have a better overlap and energy match for X = H compared to X = Rh, Ti. The larger steric destabilization for X = Ti, Rh compared to X = H reflects the larger size of the metal complexes compared to the hydrogen atom. Calculated X−R^2 bond orders[36] follow closely the trend in the corresponding X−R^1 bond energies for X = H, Rh, and Ti except in those cases where R^2 = Et, Pr, Pe, where the bond energies are very close.

4. Concluding Remarks

We have analyzed the strength of the XR bond for a number of hydrocarbyl groups (R) attached to X = hydrogen, Figure 1a, X = (CNCH$_3$)(H)(Tp)Rh, [Tp = H−B(pyrazolyl)$_3$], Figure 1b, and X = (OSi(CH$_3$)$_3$)(OSi(CH$_3$)$_3$)(NH−Si(CH$_3$)$_3$)Ti, Figure 1c, with the help of a DFT-based energy decomposition scheme[3,29] The hydrocarbyl groups included had a radical sp^3 carbon with unsaturated substituents containing aryl or olefinic bonds (R^1 = Ph-CH_2, mesityl, Me-allyl, allyl) or saturated alkyl substituents (R^2 = Me, Et, Pe, i-Pr, t-Bu), a radical carbon as part of a saturated ring (R^3 = c-Pr, c-Bu, c-Pe, c-He), or a radical sp^2 carbon (R^4 = Ph, t-Bu-vinyl, Me-vinyl,vinyl).

We found that X−R^4 bonds are stronger than their X−R^i counterparts (i = 1, 3) for X = H, Rh, and Ti, Table 1, due to modest destabilizing contributions from $\Delta E_{dist}^{R(X)}$ for X = H, Ti, Rh and ΔE_{steric} with X = H , Tables 4 and 5. The M−R^4 bonds (M = Rh, Ti), but not the H−R^4 links, are further stabilized relative to the M−R^i bonds (i = 1, 3) by $\Delta E_{orbital}$ through

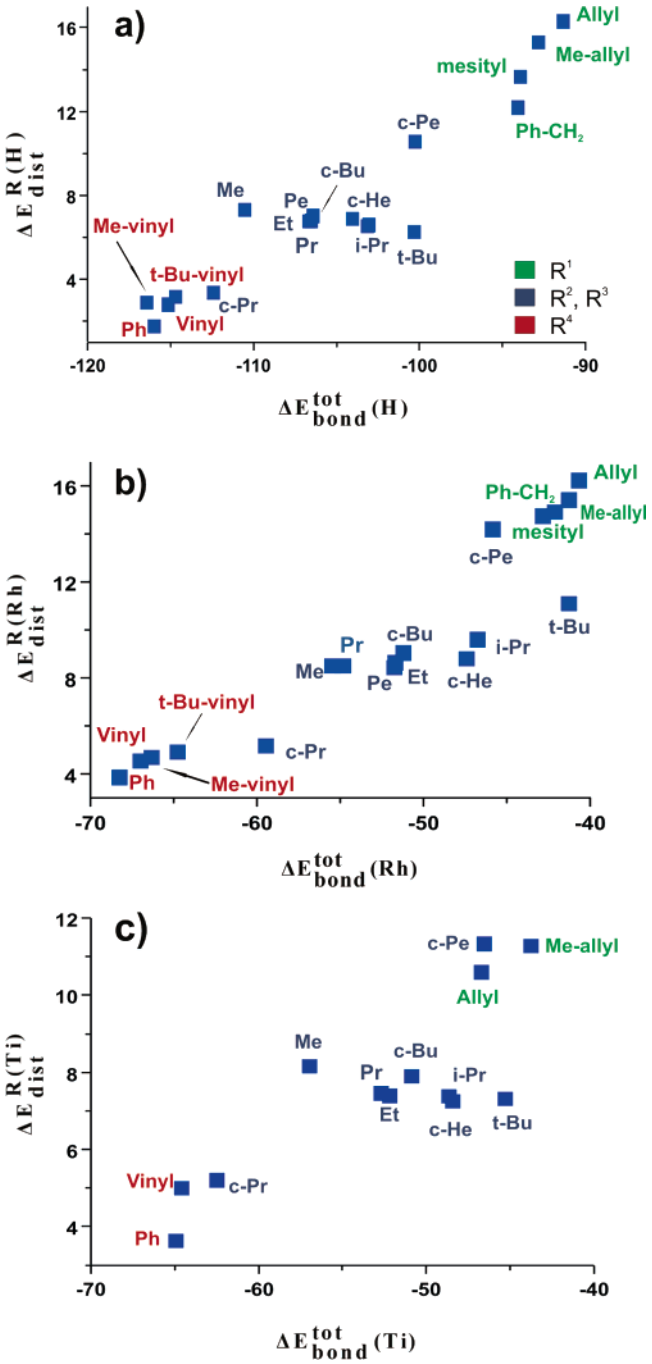

Figure 2. Correlation between radical distortion energy, $\Delta E_{dist}^{R(X)}$, and bond energy, ΔH_{bond}^{tot}(X), for X = H, Rh, Ti. All units are in kcal/mol.

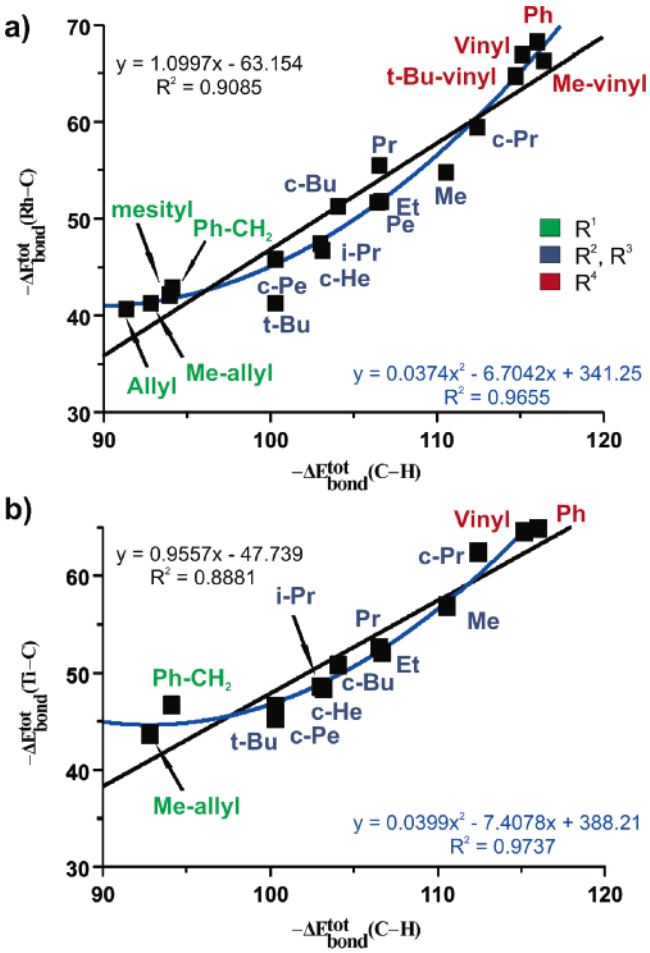

Figure 3. Correlation between the calculated ΔH_{bond}^{tot}(H) and ΔH_{bond}^{tot}(M) for M = Rh, Ti. All units are in kcal/mol.

$\Delta E_{radical}^{orb}$, Table 2. Thus, whereas the intrinsic M−R^4 ($\Delta E_{radical}^{orb}$) bonds (M = Rh, Ti) are stronger than in any other series (i = 1, 3), the intrinsic H−R^4 bonds ($\Delta E_{radical}^{orb}$) are not. In fact the HR^1 group forms the strongest intrinsic H−C bonds ($\Delta E_{radical}^{orb}$), Table 2. It is interesting to note in this connection that the difference between H−R^i and M−R^i bond energies is smallest for the XR^4 group. This might explain why H−Ph activation is more facile than one would expect from the relatively high H−Ph bond energy.

For R^3 = c-Pr, c-Bu, c-Pe, and c-He the hybridization on the radical carbon goes from sp^2 in R^3 = c-Pr to sp^3 for R^3 = c-He as the ring strain is reduced. It is thus not surprising that the X−R^3 bond energies bridge the gap between X−R^4 bonds where R^4 is sp^2 hybridized and R^1 systems with a regular sp^3 hybridization, Table 1. One trend setting factor for the X−R^3 bond energies is $-\Delta E_{radical}^{orb}$. It is seen to decrease from R^3 = c-Pr to R^3 = c-He as the hybridization of the carbon lobe in σ_{XR} changes from sp^2 to sp^3. The other factor is $\Delta E_{dist}^{R(X)}$.

The series R^2 = Me, Et, Pr, Pe, iso-Pr, and t-Bu has an average X−R^2 bond energy below that of the XR^4 group and close to that of the XR^3 series. Within the XR^2 group we find a decrease in the X−R^2 bond energy with increasing substitution on the radical carbon of R^2. The interpretation of this trend has been the subject of considerable controversy for X = H. We find in agreement with the recent suggestion by Gronert[1] and previous calculations[2] that the trend from Me to t-Bu can be explained in terms of growing 1,3 geminal repulsion between hydrogen and the substituents on the carbon bound to hydrogen, ΔE_{steric}. For the MR^2 group (M = Rh, Ti) we have a similar drop in bond energy as R^1 gets bulkier. One might thus have expected ΔE_{steric} to increase for X = Rh, Ti in a way similar to X = H. However, this is not the case. Instead ΔE_{steric} is more or less constant as the steric strain is relieved by increasing the M−C bond distance, Table 3. Instead, the decrease in the intrinsic M−C bond energy ($-\Delta E_{radical}^{orb}$) is now the trend setting factor. Thus the influence of the steric bulk for X = Rh, Ti is indirect but influencing the X−R^2 bond energy in the same direction as for X = H.

The R^1 series (R^1 = Ph-CH$_2$, mesityl, Me-allyl, allyl) forms the weakest X−C bonds. Responsible here is the steric energy term ΔE_{steric} as well as $\Delta E_{dist}^{R(X)}$ from the energy due to the distortion of the R^1 radical. The latter term is high because the

R^1 radicals are planar with substantial delocalization of the radical electron into the π^* orbitals of the aryl or olefin substituents on the radical carbon of R^1. A compensating factor is $-\Delta E^{orb}_{virtual}$ due to the donation of charge from σ_{XR} into the π^* orbitals of the aryl or olefin substituents. This term is especially large for X = H. In fact, $-\Delta E^{orb}_{radical}$ in HR^2 exceeds the value of $-\Delta E^{orb}_{radical}$ in HR^i (i = 1, 3, 4) by as much as 10 kcal/mol.

We note finally that the Rh−R and Ti−R bonds are some 47−60 kcal/mol weaker than the H−R links. There are three factors contributing to this difference, namely, $\Delta E_{orbital}$ (∼75−50%), ΔE_{steric} (∼0−30%), and $\Delta E^{Rh-frag}_{dist}$ or $\Delta E^{Ti-frag}_{dist}$ (∼20−10%). The difference between the Rh−R^1 and Ti−R^1 bond energies is, on the other hand, marginal. The more modest stabilization in $\Delta E_{orbital}$ for X = Ti, Rh compared to X = H stems from the fact that the orbitals involved in the formation of σ_{XR} have a better overlap and energy match for X = H compared to X = Rh, Ti. The larger steric destabilization for X = Ti, Rh compared to X = H (with the exception of R^2) reflects the larger size of the metal complexes compared to the hydrogen atom. M−R complexes have further distortion destabilizations ($\Delta E^{Rh-frag}_{dist}$ or $\Delta E^{Ti-frag}_{dist}$) not encountered by the HR systems. The M−R complexes tend to reduce potential steric interactions by increasing the M−R bond length for more bulky R groups, notably in the case of R^1 and R^3, at the expense of reducing the stabilizing interaction from $\Delta E_{orbital}$ through $\Delta E^{orb}_{radical}$.

We should also point out the very different nature of C−H and M−C bonds. The quantities that are used in literature[40,41] to roughly estimate the ionic and covalent bond features are electrostatic ΔE_{elstat} and orbital interaction $\Delta E_{orbital}$ terms. The average ionicity estimated from those contributions for the C−H bonds is 30.82%, whereas for Rh−C and Ti−C bonds we noticed an average ionicity of 53.02% and 50.91%, respectively. These results are in line with Harvey.[39]

It was found that the average bond energy within each group increases as $R^4 > R^3 \sim R^2 > R^1$ for the two metals as well as H. This trend correlates with the radical stabilization energy, $-\Delta E^{R(X)}_{dist}$, of R^i that decreases in absolute terms as $R^4 < R^3 \sim R^1 < R^2$. This trend enables one to make rough correlations between the strength of M−C bonds and M−H links on going from one group to another, Figure 2. Within XR^i systems where i = 1, 3, 4 there is also a correlation between the X−R^i bond energies and the R^i distortion energy, Figure 2. The practice of correlating C−X bond energies with the radical stabilization energy, $-\Delta E^{R(X)}_{dist}$, is well established[38] especially for X = H, and it is in part due to this relation that one is able to correlate C−H and M−C bond strengths as done previously by Clot[31] and again by us in Figure 3. We find the correlation for a quadratic fit to be good with a correlation factor R^2 of 0.9655 for X = Rh and 0.9735 For M = Ti. We noted also the slope values 1.0997 and 0.9557 for the rhodium and titanium complexes, respectively. The lack of agreement in slope values with the Clot et al. results[31] (1.22 and 1.08 for the X−Rh, X = Ti) can be attributed to the zero-point energy corrections and finite temperature not included in our calculations.

We note finally that trends in the X−R^2 bond energies are directly (X = H) or indirectly (X = Rh, Ti) determined by increasing steric bulk on R^2. We suspect that a similar strong dependence on increasing steric bulk within a group can be introduced for R^i (i = 1, 3, 4) by adding bulky substituents to the radical carbon as in the XR^2 series.

Acknowledgment. This work has been supported by the National Sciences and Engineering Research Council of Canada (NSERC) and partly by a research grant from the Ministry of Education and Science in Poland (1130-T09-2005-28). T.Z. thanks the Canadian Government for a Canada Research Chair.

OM0700361

(38) Gronert, S. *J. Org. Chem.* **2006**, *71*, 7045−7048.
(39) Harvey, J. N. *Organometallics* **2001**, *20*, 4887−4895.
(40) Esterhuysen, C.; Frenking, G. *Theor. Chem. Acc.* **2004**, *111*, 381−389.
(41) Frenking, G.; Wichman, K.; Fröhlich, N.; Loschen, C.; Lein, M.; Frunzke, J.; Rayón. *Coord. Chem. Rev.* **2003**, *238−239*, 55−58.